Journal of Radiation Research and Imaging

Appelbaum et al., J Radiat Res Imaging 2021; 1(1):27-32.

Commentary

Modification of circumsolar radiation for anisotropic diffuse radiation models: Photovoltaic collectors on sloped planes

Appelbaum J*, Aronescu A

School of Electrical Engineering, Tel Aviv University, Israel

*Author for correspondence: Email: appel@eng.tau.ac.il

Received date: December 21, 2020
Accepted date: February 02, 2021

Citation: Appelbaum J, Aronescu A. Modification of circumsolar radiation for anisotropic diffuse radiation models: Photovoltaic collectors on sloped planes. J Radiat Res Imaging. 2021; 1(1):27-32.

Abstract

Photovoltaic fields are deployed in multiple collector rows on horizontal and on sloped planes, therefore the second (and subsequent rows) sees the sky dome with a smaller angle than the first (front) row. A relatively large number of diffuse radiation models have been proposed based on isotropic and anisotropic models. The anisotropic models include circumsolar radiation and horizon brightening, and refer to single rows of collectors. The present article modifies the anisotropic models by two factors: (a) Sky view factor of a second row, depending on the collector and field parameters, (b) Modification to circumsolar brightening. The present article develops the modification to include collector rows deployed on sloped planes facing the south and north. The modifications are demonstrated on Klucher model for diffuse radiation. The study points out the differences in the diffuse incident irradiation on the front and on the second collector row for isotropic and anisotropic modified (Klucher) models. The study shows that for latitude 32° N and relative low percentage of diffuse radiation, the isotropic model resulted in 10.7% less annual diffuse incident irradiation as compared to Klucher original model for the front collector row. The isotropic model predicts 5.8% less annual diffuse incident irradiation compared to the proposed modified Klucher model for the second and subsequent collector rows.

Keywords: Diffuse radiation, Circumsolar radiation, Klucher model, PV collectors on sloped planes

Introduction

The isotropic and anisotropic models for diffuse radiation were developed for a single row of PV collectors. Photovoltaic (PV) fields are deployed in multiple rows on horizontal planes, on sloped planes facing south and may also be deployed on sloped planes facing north. Therefore, the second and subsequent rows are exposed to the sky dome with a smaller view angle than the first row. In addition, the collector view angle may also be different depending on plane orientation whether north or south. Obscuring part of the sky by rows in front affects the diffuse incident radiation. It should be noted that the diffuse radiation may constitute a significant component of the global radiation, depending on the location of the site. A relatively large number of diffuse radiation models have been proposed for inclined surfaces based on isotropic and anisotropic models [1-7]. Article [8] deals with the corrections to anisotropic diffuse radiation model for PV fields with multiple rows deployed on horizontal planes. The present article extends the corrections (modifications) and includes PV collectors deployed on sloped planes facing north and south. The modified model is again demonstrated on Klucher anisotropic model for diffuse radiation.

The Klucher model [3] for diffuse radiation G_d on a surface ("all sky" anisotropic model) is formulated by:

$$G_d = F_{c\to sky}\, G_{d\hat{h}}(1+F_K\cos^2\theta\sin^3\theta_Z)(1+F_K\sin^3\frac{\beta}{2}) \qquad (1)$$

where

$$F_K = 1-\frac{G_{d\hat{h}}}{G_{g\hat{h}}} = \frac{G_{g\hat{h}}-G_{d\hat{h}}}{G_{g\hat{h}}} \qquad (2)$$

$F_{c\to sky}$ is the surface sky view factor, G_{gh}, G_{dh} are the global and diffuse radiation on a horizontal surface, respectively, θ is the angle between the solar rays and the normal to the surface, and θ_z is the sun zenith.

The sky brightening near the sun (circumsolar) is termed by the factor

$$(1+F_K\cos^2\theta\sin^3\theta_z), \qquad (3)$$

and the increase in the sky radiation near the horizon is termed by the factor

$$(1+F_K\sin^3\frac{\beta}{2}). \qquad (4)$$

Two factors are modified in the present article: (a) sky view factor of a second and subsequent rows and (b) correction to circumsolar brightening. As the third term of horizon brightening of Klucher model is negligible [8], this factor was not considered.

Materials and Methods

Row distance

The sky view factor and the circumsolar brightening depend on the row distance; therefore, the row distance is calculated first for horizontal and sloped planes. The row distance in PV field may be determined by various methods [9,10]. In the present study the row distance is determined by the shadow length on Dec 21st at noon. The sun elevation angle α on that day and hour is given by [11]:

$$\sin\alpha=\sin\phi\sin\delta+\cos\phi\cos\delta_0 \ , \ \text{or}$$

$$\tan\alpha=\tan[\sin^{-1}(\cos(\phi-\delta_0))] \qquad (5)$$

Where ϕ is the site latitude and δ_0 is sun declination angle at noon on Dec 21. The row distance for a horizontal plane is therefore given by Figure 1:

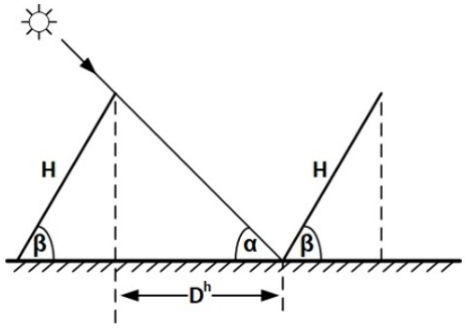

Figure 1: Horizonal plane.

$$D^h=\frac{H\sin\beta}{\tan\alpha} \qquad (6)$$

and with Equation 5:

$$D^h=\frac{H\sin\beta}{\tan[\sin^{-1}(\cos(\phi-\delta_0))]} \qquad (7)$$

For a sloped plane ε facing south (Figure 2) the row distance is:

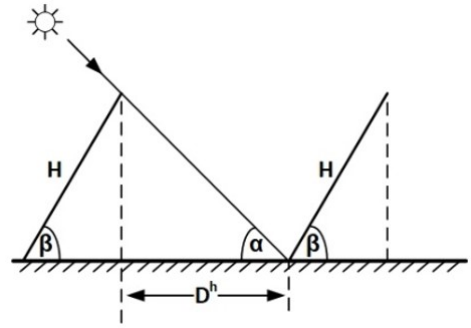

Figure 2: Sloped plane facing south.

$$D_\varepsilon^S=\frac{H\sin\beta-B^{south}}{\tan[\sin^{-1}(\cos(\phi-\delta_0))]} \qquad (8)$$

where

$$B_\varepsilon^S=(H\cos\beta+D_\varepsilon^S)\tan\varepsilon \qquad (9)$$

and by substituting in Equation 8 and solving for D_ε^S we obtain:

$$D_\varepsilon^S=\frac{H\sin\beta-H\cos\beta\tan\varepsilon}{\tan[\sin^{-1}(\cos(\phi-\delta_0)]+\tan\varepsilon} \qquad (10)$$

For a sloped plane ε facing north (Figure 3) the row distance is:

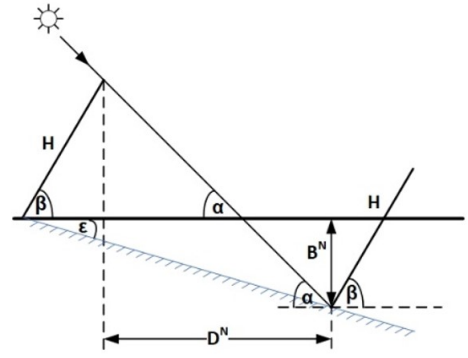

Figure 3: Sloped plane facing north.

$$D_\varepsilon^N=\frac{H\sin\beta+B^N}{\tan[\sin^{-1}(\cos(\phi-\delta_0))]} \qquad (11)$$

where

$$B_\varepsilon^N=(H\cos\beta+D_\varepsilon^N)\tan\varepsilon \qquad (12)$$

obtaining:

$$D_{\varepsilon}^{N} = \frac{H\sin\beta + H\cos\beta\tan\varepsilon}{\tan[\sin^{-1}(\cos(\phi-\delta_0)]-\tan\varepsilon} \quad (13)$$

Sky View Factor Correction

Front (first) row

The sky view factor for a collector in the first row deployed on a horizontal plane is given by:

$${}^{1}F^{h} = (1+\cos\beta)/2 \quad (14)$$

Based on "cross-string rule" by Hottel [12], the sky view factor for a collector in the second row deployed on a horizontal plane is given by [13]:

$${}^{2}F^{h} = \frac{H + D^{h} + H\cos\beta - [(D^{h})^{2} + (H\sin\beta)^{2}]^{1/2}}{2H} \quad (15)$$

The sky-view factor for a collector in the second row deployed on a sloped-plane ε facing south (S) is given in [13]:

$${}^{2}F_{\varepsilon}^{S} = \frac{H + [(D_{\varepsilon}^{S} + H\cos\beta)^{2} + (B_{\varepsilon}^{S})^{2}]^{1/2} - [(D_{\varepsilon}^{S})^{2} + (H\sin\beta - B_{\varepsilon}^{S})^{2}]^{1/2}}{2H} \quad (16)$$

where B_{ε}^{S} is given in Equation 9.

The sky-view factor for a collector in the second row deployed on a sloped-plane ε facing north (N) is obtained similarly,

$${}^{2}F_{\varepsilon}^{N} = \frac{H + [(D_{\varepsilon}^{N} + H\cos\beta)^{2} + (B_{\varepsilon}^{N})^{2}]^{1/2} - [(D_{\varepsilon}^{N})^{2} + (H\sin\beta + B_{\varepsilon}^{N})^{2}]^{1/2}}{2H} \quad (17)$$

Where B_{ε}^{N} is given in Equation 12.

Obscuring Angle *Ψ*

The correction for circumsolar radiation depends the sun altitude α and on the PV field geometric parameter H, D, β expressed by the obscuring angle ψ, Figure 4. Figure 1 shows two rows of width H inclined by an angle β on a horizontal plane. The circumsolar radiation is assumed to occupy the region of five degrees. The sun

$$\sin\alpha = \sin\phi\sin\delta + \cos\phi\cos\delta\cos\omega, \quad (18)$$

elevation angle α is given in [11]:

Where φ is the cite latitude, δ is the sun declination angle and ω is the solar time angle.

The obscuring angle ψ from the sun on the second row caused by the row in front for a horizontal deployment of collector is shown in Figure 4 and is:

$$\psi = \tan^{-1}\left(\frac{H\sin\beta}{D^{h}}\right), \quad (19)$$

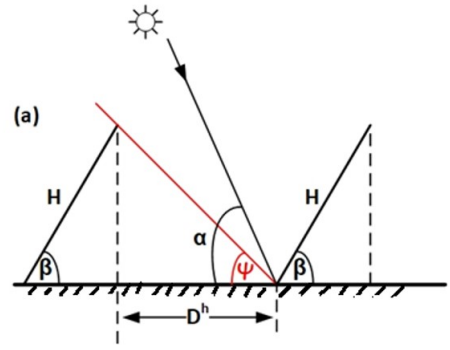

Figure 4: Obscuring angle Ψ by first row on the second row---horizontal deployment.

As long as ψ ≤ (α-2.5°) the front row is not blocking the circumsolar radiation from reaching the second row; for ψ>(α-2.5°), the circumsolar radiation is not affecting the second row.

For an inclined plane facing south, Figure 5, the obscuring angle is:

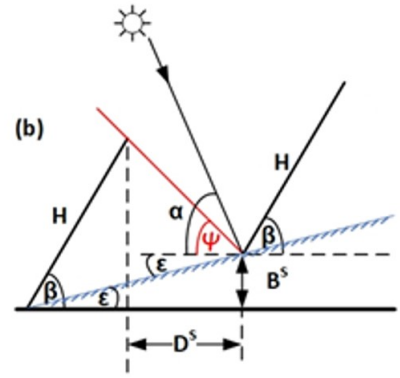

Figure 5: Obscuring angle Ψ by first row on the second row--slope facing south.

$$\psi = \tan^{-1}\left(\frac{H\sin\beta - B_{\varepsilon}^{S}}{D_{\varepsilon}^{S}}\right) \quad (20)$$

As long as ψ ≤ (α-2.5°) the front row is not blocking the circumsolar radiation from reaching the second row; for ψ>(α-2.5°), the circumsolar radiation is not affecting the second row.

For an inclined plane facing north, Figure 6, the obscuring angle is:

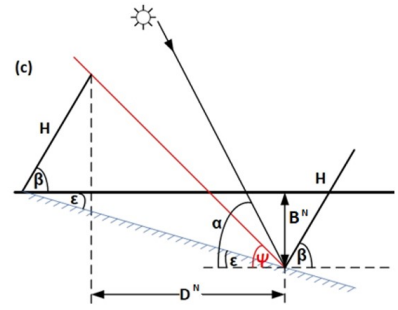

Figure 6: Obscuring angle Ψ by first row on the second row-slope facing north.

$$\psi = \tan^{-1}\left(\frac{H\sin\beta + B_{\varepsilon}^{N}}{D_{\varepsilon}^{N}}\right) \qquad (21)$$

As long as ψ ≤ (α-2.5°) the front row is not blocking the circumsolar radiation from reaching the second row; for ψ>(α-2.5°), the circumsolar radiation is not affecting the second row.

A multiple row photovoltaic field of length L=40.0m, collector width H=2.12m, inclined with an angle β=25°, ε=5°, row distance D^{h}=1.301m, $D_{\varepsilon}^{S} = 0.938m$, $D_{\varepsilon}^{N} = 1.770m$ at φ=32° N is analyzed to obtain the hours where the circumsolar radiation affects the second row (Figure 7). The calculation of the solar time striking the row surface was carried out for 21st of February, April and June, for the purpose of illustration.

Figure 7 shows, for example, that the sun rises on the first collector on 05:48 and sets on 18:12, on June 21. The sun impinges the second collector rows from 08:01 until 15:59. Because the obscuring angles ψ are equal for all three deployments (determined by the different row distance on December 21), the sun rises and sets on the same time (Figures 4, 5 and 6). The percentage of time the sun impinges the second row varies with the month and the day. For February 21, only 42.4% (4.3 hours) of the shining hours the sun strikes the second row; for April 21--58.2% (7.1 hours); and for June 21-- 64.5% (8.0 hours). Consequently, the circumsolar radiation applies to the second and subsequent rows for the appropriate times only. On December 21, the circumsolar radiation does not affect the second row at all (not shown).

Modified Klucher Model for Circumsolar Radiation

The proposed modified Klucher model for the second and for the subsequent rows includes the terms Y and the view factors, $F=F^{h}$, Equation 15; $F=F^{S}$, Equation 16, $F=F^{N}$, Equation 17. The modified anisotropic diffuse radiation model becomes:

$$G_{d} = F \times G_{dh}(1 + Y \cdot F_{K}\cos^{2}\theta \sin^{3}\theta_{Z}), \qquad (22)$$

where

$$Y = \begin{cases} 0 & \psi \geq (\alpha - 2.5^{0}) \\ 1 & \psi < (\alpha - 2.5^{0}) \end{cases} \qquad (23)$$

Comparison of Isotropic, Anisotropic Original Klucher and Modified Klucher Models

A comparison between the diffuse radiation models are applied on a multiple row photovoltaic field of length L=40.0m, collector width H=2.12m, inclined with an angle β=25°, φ=32° N (hourly solar radiation data at Tel Aviv, Israel, Israel Meteorological Service (ims)). The comparison pertains to a horizontal field and sloped fields facing south and north.

First row

Figure 8 shows variation of the annual diffuse radiation G_{d} with slope angle ε for the first row. The solid lines relate to the isotropic

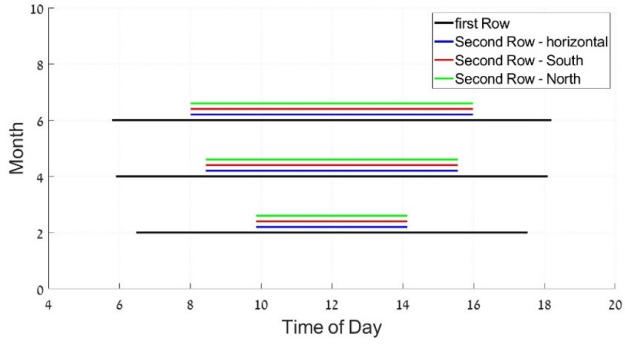

Figure 7: Hours, sun impinges on the first row (black). The sun impinges on the second row: horizontal (blue), facing south (red), facing north (green).

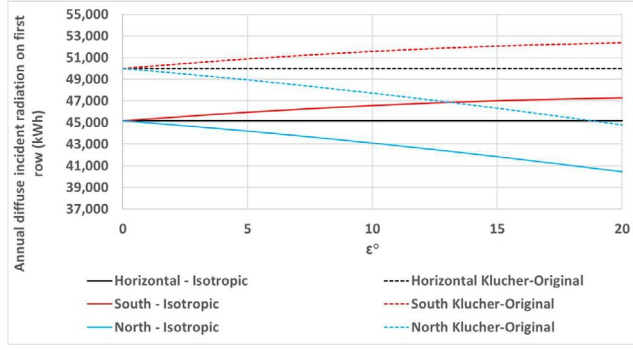

Figure 8: Annual diffuse radiation on the first row deployed on horizontal and sloped planes (south and north|) – isotropic vs Klucher original model.

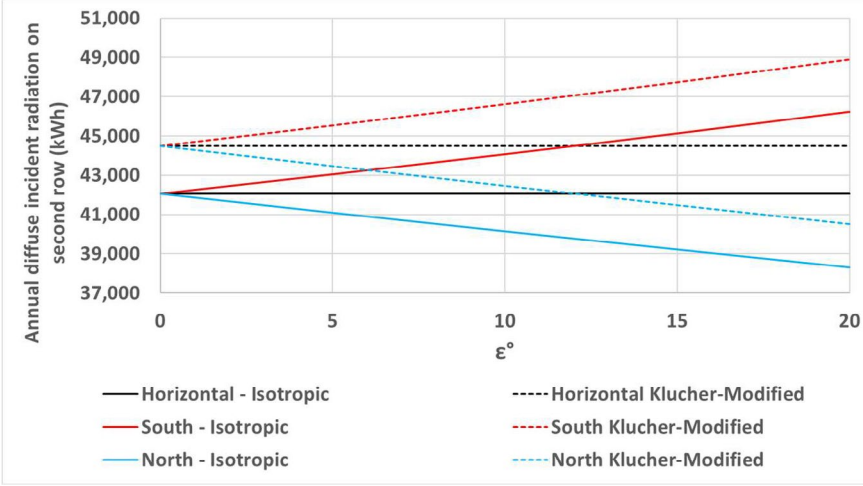

Figure 9: Annual diffuse radiation on the second row deployed on horizontal and sloped planes (south and north|) – isotropic vs Klucher modified model.

model and the dashed lines relate to the original Klucher model, Equation 1. The equations governing for the horizontal plane are: Equations 7 and 14. The equations governing for the south facing plane are: Equations 10 and 16. The equations governing for the north facing plane are: Equations 13 and 17. The comparison shows that the isotropic model for the front row underestimates by 10.7 percent the annual diffuse radiation as compared to the Klucher original model for the horizontal and for the sloped planes.

Second row

Figure 9 shows variation of the annual diffuse radiation G_d with slope angle ε for the second row. The solid lines relate to the isotropic model and the dashed lines relate to the modified Klucher model, Equation 22. The equations governing for the horizontal plane are: Equations 7 and 14. The equations governing the south facing plane are: Equations 10, 16, 22 and 23. The equations governing the north facing plane are: Equations 13, 17, 22 and 23. The comparison shows that the isotropic model for the second-row underestimates by 5.8 percent the annual diffuse radiation as compared to the Klucher modified model for the horizontal and for the sloped planes.

Discussion

Isotropic and anisotropic diffuse radiation models were developed by authors for a single row of PV collectors. However, PV fields are deployed in multiple rows on horizontal and sloped planes facing south and north. The second and the subsequent rows are therefore exposed to the sky dome with a smaller view angle than the first row. Obscuring part of the sky by rows in front affects the incident diffuse radiation. The present article extends the study in [8] and includes modification to the circumsolar brightening for PV fields on sloped planes facing south and north. Similar modification may be applied to the different anisotropic diffuse radiation models.

Conclusions

Reference [8] dealt with corrections to the anisotropic diffuse radiation model (referred to Klucher model) for PV fields deployed on horizontal planes. The present article extends that study and includes modification to the circumsolar brightening for PV fields on sloped planes facing south and north. To compare the diffuse radiation between isotropic and anisotropic models on horizontal and sloped planes, the row distance is determined by the shadow length on Dec 21st at noon for all cases studied. The study shows that for latitude 32° N and relative low percentage of diffuse, the isotropic model resulted in 10.7% less annual diffuse incident irradiation as compared to Klucher original model for the front collector row. The isotropic model predicts 5.8% less annual diffuse incident irradiation compared to the proposed modified Klucher model for the second and subsequent collector rows.

References

1. Liu BY, Jordan RC. The long-term average performance of flat-plate solar-energy collectors: with design data for the US, its outlying possessions and Canada. Solar Energy. 1963 Apr 1;7(2):53-74.
2. Hay JE. Calculation if the solar radiation incident on inclined surfaces. In Proceedings first Canadian Solar Radiation Data Workshop, Toronto. Ontario, Canada 1978.
3. Klucher TM. Evaluation of models to predict insolation on tilted surfaces. Solar Energy. 1979 Jan 1;23(2):111-4.
4. Perez R, Ineichen P, Seals R, Michalsky J, Stewart R. Modeling daylight availability and irradiance components from direct and global irradiance. Solar Energy. 1990 Jan 1;44(5):271-89.
5. Temps RC, Coulson KL. Solar radiation incident upon slopes of different orientations. Solar Energy. 1977 Jan 1;19(2):179-84.
6. Xie Y, Sengupta M. A fast all-sky radiation model for solar applications with narrowband irradiances on tilted surfaces (FARMS-NIT): Part I. The clear-sky model. Solar Energy. 2018 Nov 1;174:691-702.
7. Xie Y, Sengupta M, Wang C. A fast all-sky radiation model for solar applications with narrowband irradiances on tilted surfaces (FARMS-NIT): Part II. The cloudy-sky model. Solar Energy. 2019 Aug 1;188:799-812.
8. Appelbaum J, Massalha Y, Aronescu A. Corrections to anisotropic diffuse radiation model. Solar Energy. 2019 Nov 15;193:523-8.
9. Ma XS, Yao GH, Ye LJ, Zhi XF, Zhang SM. Distance calculation between photovoltaic arrays fixed on sloping ground. Journal of Computational Methods in Sciences and Engineering. 2015 Jan 1;15(1):107-16.

10. Maheshwari JU, Devi SJ. Impact of panel shading in the solar panel. International Journal of Advanced Research in Basic Engineering Sciences and Technology (IJARBEST). 2017; 3(36):74-77.

11. Bany J, Appelbaum J. The effect of shading on the design of a field of solar collectors. Solar Cells. 1987 Apr 1;20(3):201-28.

12. Hottel HC, Sarofin AF. Radiative Transfer. McGraw Hill, New York; 1967.

13. Appelbaum J. The role of view factors in solar photovoltaic fields. Renewable and Sustainable Energy Reviews. 2018 Jan 1;81:161-71.